scientific reports

OPEN

Sex-specific response of intramuscular fat to diet-induced obesity in rats

Hannah E. Smith[1,2 ✉], Nada Abughazaleh[1,2], Ruth A. Seerattan[1], Faizan Syed[1], Daniel Young[2], Antoine Dufour[2], David A. Hart[2], Raylene A. Reimer[1,2] & Walter Herzog[1,2 ✉]

Metabolic abnormalities associated with excess adiposity in obesity contribute to many noncommunicable diseases, including sarcopenic obesity. Sarcopenic obesity is the loss of muscle mass coupled with excess fat mass and fatty infiltrations in muscle tissue called myosteatosis. A diet-induced obesity model was developed to study fat infiltration in muscle tissue. Only male rats have been considered in these investigations neglecting that female rats might respond differently. The objective of this study was to determine if the response to diet-induced obesity can be generalized to both sexes, or whether sex affects the response to the HFS diet, as indicated by markers of metabolic syndrome and changed in muscle integrity. Using a combination of histological staining techniques, quantitative proteomics, and measures of metabolic syndrome and inflammation, it was determined that the diet-induced obesity model in female Sprague-Dawley rats is a viable model with pronounced effects on the musculoskeletal system. We found sex-dependent and muscle-specific differences in intramuscular fat infiltration between male and female rats receiving the obesogenic diet. Including females in research may allow for identifying distinct causes of the mechanistic relationship between diet, obesity, metabolic syndrome, and the sex-dependent differential effects of these factors on adaptation and degeneration of musculoskeletal tissues.

Keywords Muscle, Obesity, Metabolic syndrome, Cachexia, Sex differences, Inflammation

The World Health Organization has reported that obesity has reached epidemic levels, having tripled in the last 50 years. Western-type diets that are high in fat and sugar often lead to obesity and associated metabolic syndrome. Metabolic syndrome is characterized by the presence of a cluster of conditions which includes abdominal obesity, hypertension, dyslipidemia, and hyperglycemia, all of which put a person at a greater risk for cardiovascular disease[1]. A less well-known risk of excessive fat gain is sarcopenic obesity. Sarcopenic obesity is defined by low muscle mass and function coupled with excessive fat mass[2]. As muscle mass has been found to be positively associated with longevity[3] and other measures of quality of life[4,5], it is important to understand the relationship between diet and muscle integrity.

Myosteatosis, or fat infiltration in muscle tissue, is poorly characterized, yet is an important feature of sarcopenic obesity. Fatty infiltrations in muscle tissue in sarcopenic obesity can further exacerbate the symptoms of metabolic syndrome due to the relative loss of muscle mass to fat gain[6,7]. Studies have found intramuscular lipid accumulation to be associated with dyslipidemia, hyperglycemia, and hypertension in both men and women[6,8]. Insulin resistance is commonly increased as well, as muscle is the largest organ responsible for glucose regulation[9–11]. Furthermore, proinflammatory cytokines that circulate in the obese state can further disrupt the regenerative capacity of skeletal muscle[10]. Whereas the muscle undergoes regular remodeling triggered by inflammatory signaling[12–14], the environment created by local cytokines in obesity facilitates conditions of chronic injury leading to irregular remodeling and pathophysiologic fibrosis[15]. Furthermore, intramuscular fat infiltration and fibrosis are associated with decreased skeletal muscle contraction which can lead to a loss of muscle strength and physical function[4,5,16–19]. These conditions, in turn, are thought to encourage a sedentary lifestyle that further promotes weight gain and obesity.

To study fat infiltration in muscle tissue, a diet-induced obesity model in male Sprague–Dawley rats was previously developed. It has been demonstrated that a high fat/high sucrose (HFS) diet induces obesity and low-grade systemic and local muscle inflammation in this pre-clinical model[20,21]. The HFS diet led to an increase in fat infiltration and fibrosis in the primarily fast twitch fibred vastus lateralis (VL) muscle in as early as three days

[1]Human Performance Lab, University of Calgary, Calgary, AB, Canada. [2]McCaig Institute for Bone and Joint Health, University of Calgary, Calgary, AB, Canada. ✉email: hannah.smith@ucalgary.ca; wherzog@ucalgary.ca

following the start of a metabolic challenge[20]. However, the oxidative capacity of the soleus muscle (~ 100% slow twitch fibred in Sprague Dawley rats)[22] seemed to protect against changes in muscle integrity[23].

Pre-clinical studies on obesity-induced metabolic disease and associated changes in muscle health have used male animals, as males are typically thought to have a steady metabolic profile, while females undergo periodic cycles of metabolic profiles associated with their pup-bearing function. Up to this point, studies looking at obesity related musculoskeletal degeneration in rats have only been performed in males. As females can differ in the presentation and mechanism behind various diseases[24,25], it is important to understand the impact that sex has on musculoskeletal health. Furthermore, studying male and female rats may provide unique opportunities to understand the different relationships that may exist between metabolic responses to an obesogenic diet and corresponding musculoskeletal adaptations and degenerations.

Therefore, the purpose of the present study was to determine if previous findings from the model of diet-induced obesity in male rats can be generalized to both sexes, or whether sex affects the response to the HFS diet, as indicated by markers of metabolic syndrome and changes in muscle integrity. We assessed the VL and soleus muscle in male and female Sprague Dawley rats after a 12-week HFS diet intervention using muscle histology and a quantitative proteomics analysis as our primary outcomes. It was hypothesized that the structural changes in the muscles associated with the HFS diet intervention would be similar in the male and female rats. However, we detected sex-dependent and muscle-specific differences in intramuscular fat infiltration between male and female rats receiving the obesogenic diet.

Methodology
Experimental design
The current study is reported in accordance to ARRIVE guidelines. Twenty-four male and twenty female Sprague–Dawley rats were housed in pairs on a 12-h dark/light cycle. All animals were purchased from the University of Calgary's Life and Environmental Science Animal Research Centre where they were bred and raised according to Canadian guidelines. Within each sex, rats were either allocated to a HFS diet group (39.2% of total energy as fat, 43.5% sucrose, 15.8% protein; custom Diet #102412, Dyets, Inc, n = 12 males, n = 12 females) or to a chow control diet (Chow, 13.4% of total energy as fat, 3.8% sucrose, 29.8% protein, Lab Diet 5001, n = 12 males, n = 8 females). All experiments were approved by the University of Calgary Life and Environmental Sciences Animal Care Committee, and experiments were conducted in accordance with the Canadian Council on Animal Care standards. The animals were 12 weeks old at the start of the ad libitum diet intervention. All animals remained on the diet for 12 weeks and were euthanized at 24 weeks of age. Animals were anesthetized with isoflurane and then euthanized by a cardiac blood draw and aortic snip. Prior to euthanasia, body mass and composition were measured using Dual Energy X-ray Absorptiometry (DXA) and analyzed with software for small animal analysis (GE Lunar DXA).

Muscle characterization
The VL and soleus muscles were harvested and flash-frozen in liquid nitrogen and stored at minus 80 °C until analysis. Myosin heavy chain (MHC) isoforms from both muscles were identified using SDS-PAGE with a 7.5% acrylamide separating and 4.5% stacking gel as previously described by Joumaa et al[26]. The electrophoresis was performed using a Bio-Rad (USA) Mini-Protean unit with 0.75 mm spacer plates at a constant voltage of 73 V for 18 h followed by a constant current of 1.5 mA/gel for 23.5 h at 4 °C. Gels were stained with Coomassie brilliant blue and imaged using a GS-800 Calibrated Densitometer (Bio-Rad, USA). Quantification of the band optical density was performed using ImageJ[27], and proportions of MHC IIa, IIx, IIb, and I were determined in terms of total MHC content of the muscle.

Cytokine, adipokine, and blood lipid profile measurements
Following an overnight fast, blood was collected immediately following anesthesia via cardiac puncture. Samples were centrifuged at 7000 rpm for 15 min, and two serum aliquots stored at -80°C until analysis. One sample was used to quantify twenty-seven serum cytokines and adipokines using a Rat Cytokine/Chemokine 27-Plex Discovery Assay Array (Eotaxin, EGF, Fractalkine, IL-1α, IL-1 β, IL-2, IL-4, IL-5, IL-6, IL-10, IL-12(p70), IL-13, IL-17A, IL-18, IP-10/CXCL10, GRO/KC, IFN-γ, TNF-α, G-CSF, GM-CSF, MCP-1, leptin, LIX, MIP-1α, MIP-2, RANTES, vascular endothelial growth factor (VEGF), Eve Technologies, Calgary, AB). The other serum sample was analyzed for lipid profile (total cholesterol, LDL-cholesterol, HDL-cholesterol, and triglycerides) using colorimetric assays (Calgary Lab Services, Calgary, AB, Canada).

Insulin sensitivity analysis
One week before sacrifice, animals underwent an insulin sensitivity test. Animals were fasted for 14 h prior to blood collection. Blood was collected via tail nick in a chilled tube for insulin analysis. Blood glucose was measured immediately with a blood glucose meter (OneTouch Verio and Blood Glucose Monitoring System, Lifescan, Switzerland). Insulin resistance was calculated using the HOMA-IR index which uses the fasted blood glucose concentration and insulin levels (homeostatic model assessment for insulin resistance—HOMA-IR[28]. A value higher than 2.5 is indicative of increased insulin resistance in humans.

Histological staining procedures
Slide preparation
A 3 mm mid-belly slice of the previously flash-frozen muscle was cut, mounted on OCT compound and sectioned at 10 μm using a Leica cryostat at – 20 °C, dried at room temperature, and then stored in – 20 °C until used. Oil Red O (ORO) staining for intramuscular fat, Picrosirius red staining for collagen/fibrosis, and CD68+ immunohistochemistry was completed on one slide per staining procedure.

Oil red O staining
As previously described by Collins et al. (2016), ORO stock solution was made by adding 2.5 g Oil Red O (Sigma-Aldrich, Oakville, ON, Canada) to 400 mL of 99% isopropanol (Fisher Scientific, Ottawa, ON, Canada). ORO working solution was then prepared from a ratio of three parts ORO stock: two parts distilled water and was filtered using a course filter, then was refrigerated at 4 °C for 10 min before use. Sections were first washed quickly in distilled water and then quickly dipped in 60% isopropanol and stained for 20 min in the ORO working solution. Slides were then rinsed first in 60% isopropanol and then in distilled water, and finally cover-slipped with glycerol jelly.

Picrosirius red staining
Slides were dried for 2 weeks in a 38 °C oven, fixed overnight in neutral buffered formalin (NBF) and then immersed in Bouin's fixative solution for 1 h at 60 °C in a water bath, and then washed in distilled water. The Picrosirius red solution was made by adding 0.1 g of Sirius red stain (Sigma-Aldrich), to 100 mL of a saturated aqueous picric acid (1.3% in water, Sigma-Aldrich). Sections were left in this solution to stain for 1 h at room temperature and then rinsed in 2 changes of 1% acetic acid, dehydrated in three changes of 100% ethanol, cleared in 2 changes of xylene, and mounted with Cytoseal 60 mounting media (Collins et al. 2016).

Stain quantification
ORO and Picrosirius red stained sections were imaged at 40× magnification with an Olympus DP73 camera mounted on an Olympus BX53, and the corresponding images were analyzed using the software ImageJ (Rasband, WS, ImageJ, U.S. National Institutes of Health, Bethesda, Maryland, USA). Images were taken of the entire muscle section and were quantified by one reviewer who was unaware of which diet group each muscle section belonged to. The relative percentage of intramuscular fat and fibrosis was determined per cross sectional area of the muscle.

Immunofluorescence
Immunofluorescence was performed as described previously[29]. In brief, slides were first fixed in cold acetone for 30 min, quenched for 20 min in 3% hydrogen peroxide, and then blocked using 2.5% normal horse serum (Vector Laboratories, Burlingame, CA). Sections were then incubated overnight at 4 °C with the primary antibody, mouse anti-rat CD68^{+}, a marker for inflammatory macrophages, at a dilution ratio of 1:200. The secondary antibody, IMPRES anti-mouse IgG peroxidase (IMPRESS kit, Biolynx Inc) was applied the next morning for 30 min at room temperature (IMPRESS kit, Vector Laboratories). Slides were then incubated for 20 min in a Tyramide Plus Cyanine 3 Amplification system from AKOYA Biosciences. To visualize nuclei that were present in the muscle section, DAPI was applied, and sections were mounted in Vectashield mounting media for fluorescence (Vector Laboratories). All washes were performed in Phosphate buffered saline (PBS). Ten images per soleus cross-section and 20 images per VL cross-sections were obtained using an Olympus BX51 fluorescent microscope, with appropriate filters for cy3 and DAPI, and attached to an Olympus DP28 camera.

Statistical analysis
All statistical analyses were performed using R statistical software (v. 4.2.1, R Core team). Non-parametric Mann–Whitney U tests were performed on data pertaining to body composition and markers of metabolic syndrome to determine a difference between the chow and HFS animals for both sexes. A two-way ANOVA was performed to determine the main effects of Diet and Sex and their interaction, Diet × Sex, on MHC isoform distributions and histological measures. If a significant interaction effect was found, a one-way ANOVA with Tukey's post-hoc test was performed to determine differences between groups. Sex-dependent effects were not looked at for the serum cytokines because of unusual results from the male-chow animals. Instead, Mann–Whitney U tests were performed to determine differences between the chow and HFS animals for both sexes. Least-square linear regressions were used to determine if there was a relationship between body fat percentage and intramuscular fat percentage in both the male and female VL and soleus.

Proteomics
Shotgun proteomic analysis
Shotgun proteomics were carried out as described previously by[30–32] and was performed on the previously described flash-frozen VL and soleus muscle tissue that was stored at -80 °C after sacrifice of the animals. Muscle samples were added to a lysing tube with 500 uL of lysis buffer (2% SDS, 200 mM ammonium bicarbonate, protease inhibitor tablets) and 4–5 small stainless steel homogenizing beads. Samples were homogenised at 30 Hz for 20 min in the homogenizer and then sonicated with a Fisherbrand™ Model 120 Sonic Dismembrator. After sonication, samples were centrifuged at 14,000×g for 15 min at 4 °C to pellet unwanted debris and the supernatant fraction transferred into a protein lobind Eppendorf tube. Total protein concentrations for each sample were then determined using a ThermoFisher BCA kit.

Samples for the proteomic analysis were prepared using the filter-assisted separation of peptides (FASP) method. Initially, 100 µg of protein was precipitated by adding trichloroacetic acid (TCA) followed by an incubation on ice. Samples were then centrifuged at 14,000 ×g for 15 min at 4 °C, washed 3 times in ice cold acetone, and stored at − 20 °C. Samples were resuspended in 8 M tris-urea solution by shaking and then denatured with the addition of 10 mM DTT at 37 °C for 30 min. 50 mM iodoacetamide was added in the dark at room temperature to complete carbamidomethyl modification of the cysteines. Samples were moved to the top of a 30 kDa filter along with 100 uL of wash solution and were then centrifuged at 14,000×g for 15 min. Samples were then washed 3 times with 8 M tris-urea and 3 times with 50 mM ammonium bicarbonate. The samples were trypsinized at 37 °C overnight at a ratio of 1:10 trypsin: total protein, and subsequently, eluted off the filter

membrane by washing 3 times with 50 mM ammonium bicarbonate. Finally, samples were subjected to a c18 clean up with Waters solid-phase extraction (SPE) column, according to the manufacturer's directions, before injection on the orbitrap mass spectrometer in DDA mode.

High performance liquid chromatography (HPLC) and mass spectrometry
Samples were then subjected to liquid chromatography and tandem mass spectrometry at the Southern Alberta Mass Spectrometry Facility at the University of Calgary. Using a process previously described by[31–34], tryptic peptides were analyzed on an Orbitrap Fusion Lumos Tribrid mass spectrometer (Thermo Scientific) operated with Xcalibur (version 4.4.16.14) and coupled to a Thermo Scientific Easy-nLC (nanoflow Liquid Chromatography) 1200 system. Tryptic peptides (2 µg) were loaded onto a C18 trap (75 µm × 2 cm; Acclaim PepMap 100, P/N 164946; ThermoScientific) at a flow rate of 2 µL/min of solvent A (0.1% formic acid in LC–MS grade water). Peptides were eluted using a 120 min gradient from 5 to 40% (5% to 28% in 105 min followed by an increase to 40% B in 15 min) of solvent B (0.1% formic acid in 80% LC–MS grade acetonitrile) at a flow rate of 0.3 µL/min and separated on a C18 analytical column (75 µm × 50 cm; PepMap RSLC C18; P/N ES803; ThermoScientific). Peptides were then electrosprayed using 2.1 kV voltage into the ion transfer tube (300°C) of the Orbitrap Lumos operating in positive mode. The Orbitrap first performed a full MS scan at a resolution of 120,000 FWHM to detect the precursor ion having a m/z between 375 and 1,575 and a + 2 to + 7 charge. The Orbitrap AGC (Auto Gain Control) and the maximum injection time were set at 4×10^5 and 50 ms, respectively. The Orbitrap was operated using the top speed mode with a 3 s cycle time for precursor selection. The most intense precursor ions presenting a peptidic isotopic profile and having an intensity threshold of at least 5,000 were isolated using the quadrupole and fragmented with HCD (30% collision energy) in the ion routing multipole. The fragment ions (MS^2) were analyzed in the ion trap at a rapid scan rate. The AGC and the maximum injection time were set at 1e4 and 35 ms, respectively, for the ion trap. Dynamic exclusion was enabled for 45 s to avoid the acquisition of same precursor ion having a similar m/z (plus or minus 10 ppm).

Proteomic data and bioinformatics analysis
Spectra data were matched to peptide sequences from a Rat FASTA reference file obtained from Uniprot on Sept 23rd, 2020 using MaxQuant (v.2.4.9.0). Variable modifications included Oxidation on Methionine, Acetylation on any N-terminus, and Deamidation on Asparagine and Glutamine. Samples were re-quantified and matched between runs. The first search peptide tolerance was set to 10, the minimum peptide length was set to 5, and the maximum mass was set to 6,600 Da, and the minimum score for the modified peptides was set to 20. All other settings on the MaxQuant were set to default.

Statistical analysis was performed on MSstatsShiny UI (v0.1.0; https://msstatsshiny.com/app/MSstatsShiny) running MSstats (v.4.2.0). The MaxQuant files "ProteinGroups" and "evidence" were used for the analysis, while the annotation file was created according to directions provided by MSstats[35]. Unique peptides were included in the analysis. For data processing, log2 was defined for data transformation and equalize medians was the method chosen for normalization. The options "Use all features", "assume all NA as censored", "Do not apply cutoff to censor missing values", and "Model based imputation" were enabled. Statistical inference was performed using non-paired t-tests, and the data were imported to excel for final assessment. Significant enriched proteins for each group were found by separating upregulated and downregulated proteins on a log twofold change, where positive values were upregulated, and negative were downregulated. A cut-off using a p-value of 0.05 was used to determine significance. Metascape analysis was used to identify enriched pathways[36]. Protein–protein interactions were encoded into networks using the metascape website (https://metascape.org/), and enriched pathways were plotted as heatmaps.

Results
Body composition and markers for metabolic syndrome
Animals of both sexes, fed the HFS diet demonstrated a statistically higher percentage of body fat and more body mass than did the chow control animals (Fig. 1A,B, $p < 0.001$). With respect to the blood lipid profile, both male and female animals had a significant increase in blood triglycerides while on the HFS diet compared to the control group animals on the chow diet (Fig. 1C, $p = 0.008$ and $p = 0.003$, respectively). However, only the female animals on the HFS diet had a significant increase in total cholesterol and HDL cholesterol compared to the chow-fed animals (Fig. 1D,E, $p = 0.022$ and $p = 0.047$, respectively), while the males exhibited no change in total and HDL cholesterol (Fig. 1D,E, $p = 0.95$ and $p = 0.62$, respectively). Both male and female HFS diet animals had statistically higher HOMA-IR indexes than their sex-matched chow-fed controls (Fig. 1F, $p = 0.033$ and $p = 0.004$, respectively). However, there was considerable variability in the development of insulin resistance in response to the HFS diet for both male and female animals (Fig. 1F).

MHC isoform distribution
Vastus lateralis
The two-way ANOVA analysis of the MHC IIx showed a statistically significant main effect of Sex ($F_{(1,29)} = 5.79$, $p = 0.023$) and the interaction of Diet × Sex ($F_{(1,29)} = 5.54$, $p = 0.025$.) indicating the percentage of MHC IIx may be influenced by both diet and sex (Fig. 2A). Tukey's post-hoc evaluation revealed that the percentage of MHC IIx was significantly higher in the male chow-fed animal than in the female chow-fed animals ($p = 0.011$; Fig. 2A). The two-way ANOVA indicated that there was a Sex × Diet interaction effect for the percentage of MHC IIb ($F_{(29,1)} = 5.78$, $p = 0.023$). However, follow up post-hoc tests did not show any significant differences between the groups.
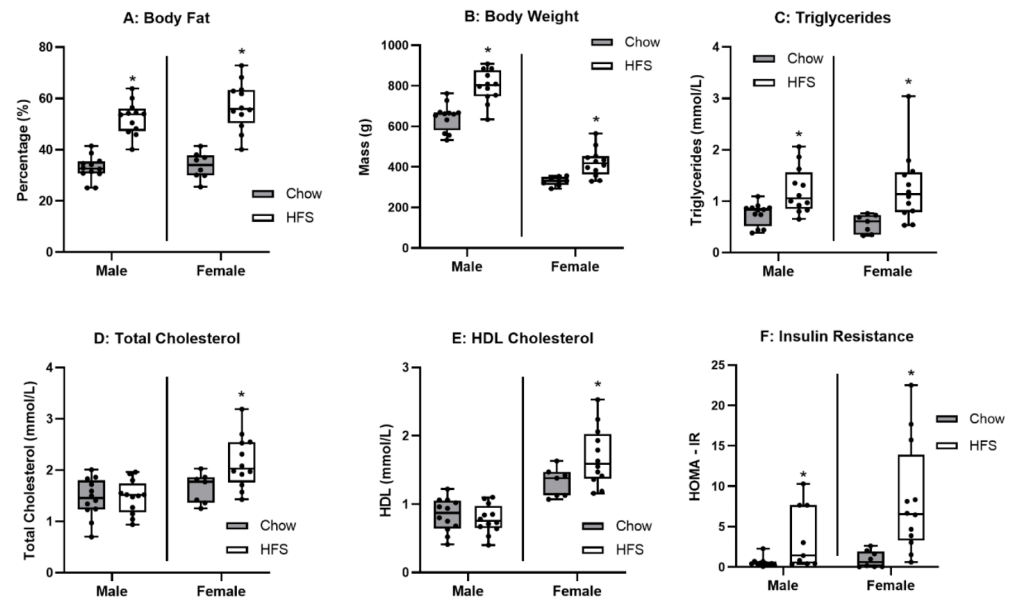
Fig. 1. Markers of metabolic syndrome for both male and female animals at the end of the diet intervention protocol for rats in the chow and HFS-fed groups. All indicators of metabolic syndrome in female animals were found to be increased in the HFS group compared to the chow-fed controls. For male animals, all values were elevated except for total cholesterol and HDL cholesterol in the HFS animals compared to the controls. *Indicates statistical significance to the level of $p < 0.05$ compared to the chow-fed animals. Data are shown in box and whisker plots where the line across the box represents the median, and the whiskers extending from the bottom and top of the box represent the minimum value to the lower quartile and the upper quartile to the maximum value respectively.
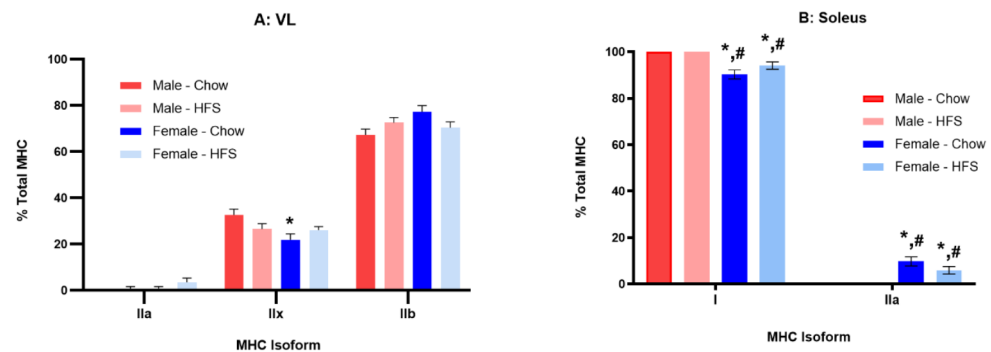

Fig. 2. Myosin heavy chain (MHC) isoform distribution in VL and soleus muscles of male and female rats fed both a chow-control diet and a HFS diet. *Indicates statistical significance to the level of $p < 0.05$ compared to the chow-fed male animals. #Indicates statistical significance to the level of $p < 0.05$ compared to the HFS-fed male animals. Error bars represent standard error of the mean.

Soleus

For the soleus muscle, the two-way ANOVA revealed a significant effect of Sex for the percentage of both MHC type I ($F_{(1,28)} = 38.42$, $p < 0.001$) and MHC IIa ($F_{(1,28)} = 38.42$, $p < 0.001$). Diet was not found to affect MHC isoform distribution in the soleus muscle. Follow-up Tukey's post-hoc tests revealed that the percentage of MHC I was significantly higher in all male compared to the female animals and MHC IIa was significantly higher in all female animals compared to the male animals, irrespective of their diet ($p = 0.011$, Fig. 2B).
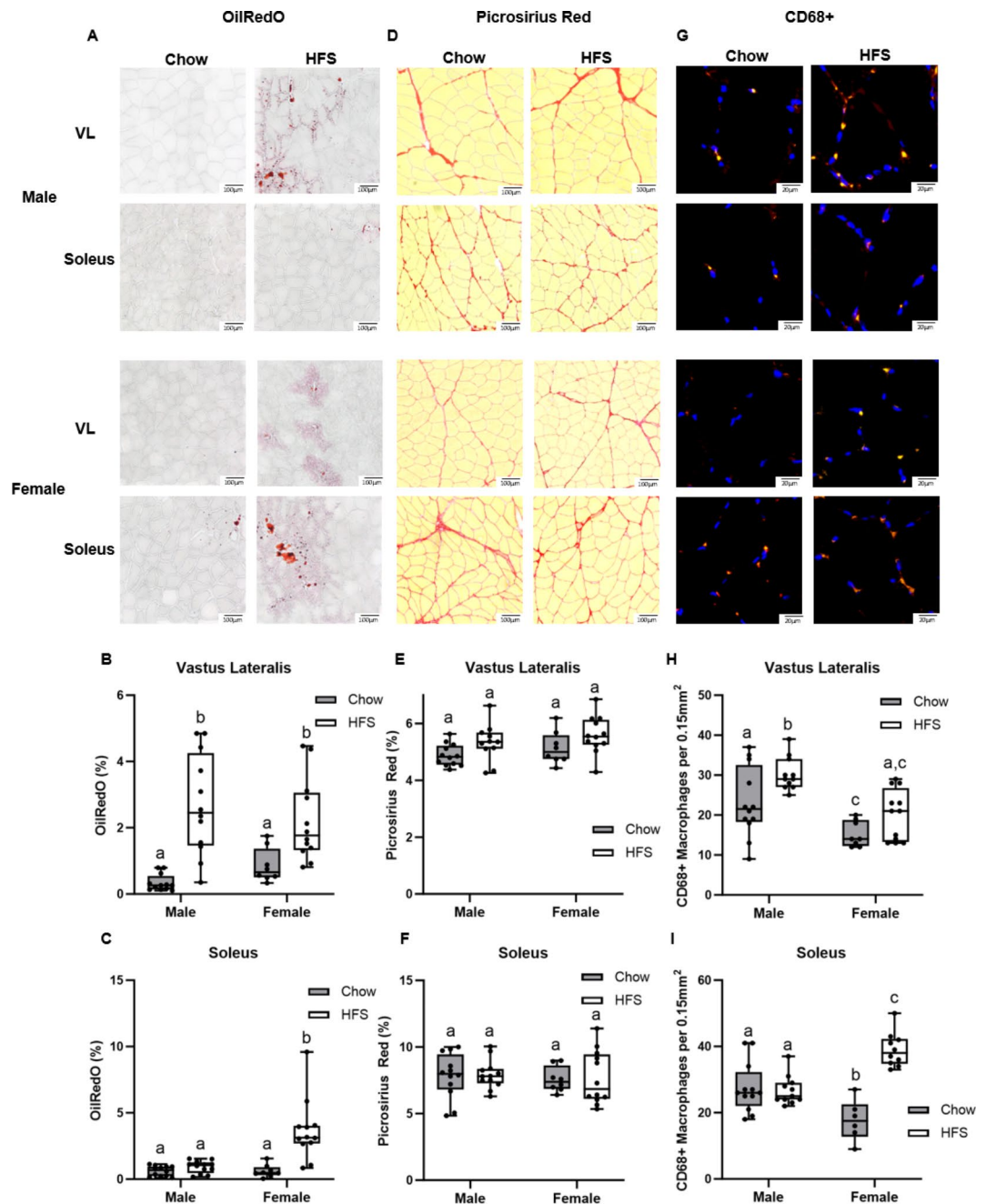
Vastus lateralis and soleus morphological changes

Vastus lateralis

The two-way ANOVA analysis showed a statistically significant main effect of Diet ($F_{(1,41)} = 33.932$, $p < 0.001$) but not Sex ($F_{(1,41)} = 0.015$, $p = 0.902$) on the intramuscular fat infiltration, represented by the % ORO staining, in the VL muscle (Fig. 3A). A Tukey's post-hoc evaluation revealed that both the male and female HFS-fed animals had significantly higher intramuscular fat infiltration than their chow-fed counterparts (Fig. 3B) ($p < 0.05$). Similarly, the two-way ANOVA indicated a significant main effect of Diet ($F_{(1,39)} = 7.478$, $p = 0.009$) but not Sex ($F_{(1,39)} = 2.285$, $p = 0.139$) on the collagen content in the VL muscle, as represented by the % Picrosirius Red staining (Fig. 3D). However, post-hoc analysis did not show any meaningful differences between groups (Fig. 3E). In terms of a macrophage response to the HFS diet in the VL muscle, a two-way ANOVA determined that both Diet ($F_{(1,39)} = 6.855$, $p = 0.013$) and Sex ($F_{(1,39)} = 22.392$, $p < 0.001$) had a significant main effect on macrophage infiltration, as represented by macrophage count per image frame (0.15 mm^2) (Fig. 3G). Tukey's post-hoc analysis revealed that macrophage count was significantly higher in chow-fed males compared to chow-fed females ($p = 0.043$), and higher in HFS-males compared to HFS-females ($p = 0.002$, Fig. 3H). There was no difference in macrophage number between chow-fed females and HFS-fed females ($p > 0.05$, Fig. 3H).

◄**Fig. 3.** Histological assessments of the VL and soleus muscle in control diet (chow) and HFS diet group rats at 24-week-old and following 12 weeks of HFS diet exposure for the experimental male and female Sprague–Dawley rats. (**A**) Oil Red O staining for intramuscular lipids in VL and soleus muscle sections in male and female animals taken at 100× magnification. (**B**, **C**) raw values for % Oil Red O staining per cross-sectional mid-belly muscle area represented by box and whisker plots. (**B**) intramuscular fat in the VL was increased after 12-weeks in the HFS diet compared to the chow control animals for both male and females (**C**) intramuscular fat in the soleus only increased in the female HFS animals following the 12-week metabolic challenge. (**D**) Picrosirius Red staining for collagen in both VL and soleus muscle sections in male and female animals taken at 100× magnification. (**E**, **F**) raw values for % Picrosirius Red staining per cross-sectional muscle area represented by box and whisker plots. No statistically significant difference was found in % Picrosirius Red staining between groups for both the VL and soleus muscle. (**G**) Immunohistochemistry staining for CD68 + cells in VL and soleus muscle sections, imaged at 200× magnification. Yellow/red CD68 + stain overlapping with blue DAPI stain, indicates the presence of a macrophage. (**H**, **I**) raw values for CD68 + macrophage count per image frame (area of $0.15mm^2$) for each animal, where 15–20 (VL) or 6–8 (soleus) images were randomly selected and evaluated for a given mid-belly muscle cross-section. (**H**) Shows that the macrophage counts in the VL muscle increased in chow-fed males compared to chow-fed females and increased the HFS-fed males compared to HFS-fed females ($p < 0.05$). No change in macrophage count was observed between chow-fed females and HFS-fed females (**I**) Shows that the macrophage response in the soleus muscle increased in the chow-fed males compared to the chow-fed females and increased in the HFS-females compared to the HFS-fed males to the HFS diet. No change was observed in macrophage count between the chow-fed male and HFS-fed male groups. Groups without a common letter are significantly different ($p < 0.05$).

Soleus

For the soleus muscle, the two-way ANOVA revealed a statistically significant main effect of Diet ($F(1,40) = 19.52$, $p < 0.001$), Sex ($F(1,40) = 15.87$, $p < 0.001$), and Diet × Sex interaction ($F(1,40) = 12.82$, $p < 0.001$) indicating that the level of the effect of the HFS diet on intramuscular fat infiltration in the soleus muscle is dependent on the sex of the animal (Fig. 3A,C). The Tukey's post-hoc test showed that the percent ORO staining in the HFS-female group was higher compared to all other groups ($p < 0.05$). No main effect differences were found in the collagen content in the soleus muscle ($p > 0.05$) (Fig. 3D,F). According to the two-way ANOVA, macrophage count in the soleus muscle varied in response to Diet ($F(1,35) = 18.88$, $p < 0.001$) and a Diet × Sex interaction ($F(1,35) = 30.971$, $p < 0.001$) indicating that the amount of macrophage infiltration is dependent on both Diet and Sex (Fig. 3G,I). Tukey's post-hoc analysis revealed that the macrophage count in the chow-males was significantly higher than the chow-fed females ($p < 0.05$, Fig. 3I). However, the HFS-fed females had a significantly higher macrophage count compared to all other groups ($p < 0.05$, Fig. 3I). There was no change in macrophage number observed between the chow-fed male and HFS-fed male groups ($p > 0.05$, Fig. 3I).

Relationship between body fat and intramuscular fat

For both male and female animals there was a significant positive relationship between body fat percentage and intramuscular fat in the VL muscle (Fig. 4A,C; males: $R^2 = 0.71$, $p < 0.001$; females $R^2 = 0.61$, $p < 0.001$). For the soleus muscle, there was a significant relationship between body fat percentage and intramuscular fat for both females and males (Fig. 4D,B; females $R^2 = 0.52$, $p < 0.001$; males $R^2 = 0.20$, $p = 0.03$).

Serum cytokines

Both male and female HFS diet animals had a statistically higher percentage of serum leptin levels compared to the chow-fed controls (Fig. 5A). For the male animals, all other serum cytokine levels were higher in the chow animals than in the HFS animals (Fig. 5B–D, $p < 0.05$). For the female animals, the HFS diet group exhibited similar serum cytokine levels to the controls for MCP-1 and IL-6 (Fig. 5B,D, $p > 0.05$). However, TNFα levels in female animals consuming the HFS diet were higher compared to the chow-fed animals (Fig. 5C, $p = 0.05$). Additional serum cytokine data can be found in Supplementary Table S3.

Quantitative proteomics analysis of muscle proteins

The proteomes of the male and female soleus and VL muscles were analyzed to determine whether their response to the HFS diet differed (Fig. 6A). In the proteomics analysis for the VL muscle (Supplementary Table S1), 95 unique proteins were identified that were upregulated in the female HFS-fed animals and 104 unique proteins that were upregulated in the male HFS-fed animals compared to the sex-matched chow control animals. Using the online meta-analysis tool, Metascape[36], several enriched pathways between HFS-fed females and HFS-fed males were identified. Male animals fed the HFS diet showed enrichment in the "innate immune system" pathway in the VL muscle compared to chow control animals (Fig. 6B). In the proteomics analysis for the soleus muscle, 463 unique proteins were identified that were upregulated in the female HFS-fed animals and 90 unique proteins that were upregulated in the male HFS-fed animals compared to the sex-matched chow control animals (Supplementary Table S2). Using Metascape, several enriched pathways were identified including innate immune system and cytokine signalling in the immune system of the soleus muscle (Fig. 6C). The quantitative proteomics analysis indicates key biological differences between male and female VL and soleus muscles.
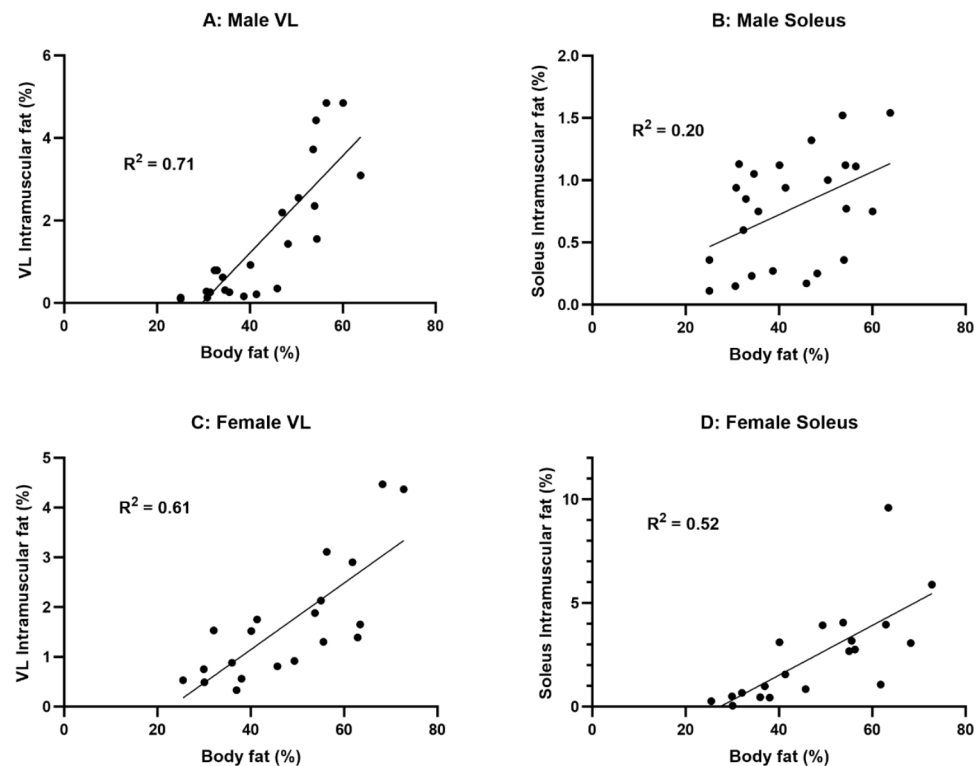
Fig. 4. Relationships between body fat percentage and intramuscular fat percentage in the VL and soleus muscle in male and female rats. The corresponding R^2 values are shown on the figures. Medium to strong relationships were found between body fat percentage and intramuscular fat infiltration for male VL and female VL and soleus ($p < 0.05$).

Discussion

The link between obesity and the decline in muscle integrity, classified by the increase in intramuscular lipid content and fibrosis, has been previously well established[19–21,23,37–39]. However, previous studies failed to consider female models of diet-induced obesity. The aim of the current study was to determine if previous findings from the model of diet-induced obesity in male rats can be generalized to both sexes, or whether sex affects the response to the HFS diet, as indicated by markers of metabolic syndrome and changes to muscle integrity. An important finding from this study was that female Sprague–Dawley rats became obese and showed symptoms consistent with metabolic syndrome after 12-weeks on the HFS diet. Similar to the male animals, female animals exposed to the HFS diet displayed a significant increase in body fat percentage, elevated blood triglycerides, and increased insulin resistance (Fig. 1). However, female animals on the HFS diet also experienced an increase in HDL cholesterol levels where males did not. It has been well established in previous literature that estrogen is associated with an increase in HDL cholesterol[40]. Exposure to the HFS diet also resulted in various effects of both diet and sex on intramuscular fat infiltration, fibrosis, and macrophage invasion in the VL and soleus muscles. The most notable finding was the significant increase in intramuscular fat in the soleus muscle for the female animals on the HFS diet, compared to all the other experimental groups.

Overall, the MHC isoform distribution results did not indicate that there were MHC isoform distribution changes in response to the HFS diet challenge. Although the two-way ANOVA analysis revealed an interaction effect between Diet and Sex in the VL muscle, post-hoc analysis only identified the male chow-fed animals to be different from the female chow-fed animals (Fig. 2A). It has been shown that male mice exposed to a HFS diet had a fibre type change from type I to type I/IIa hybrid. However, this result was obtained using histology and SDS-PAGE on single muscle fibres and after mice had been fed an obesogenic diet for approximately a year[41]. It is possible that co-expression of MHC isoforms within fibres was missed in our study because SDS-PAGE was performed on whole muscle samples. However, MHC transitions are slow processes and 12-weeks on the HFS diet was potentially too short a time to observe a change in MHC expression. The soleus muscle showed distinct differences in composition between the male and female animals in both diet groups (Fig. 2B). It has been reported previously that the soleus muscle in adult Sprague Dawley rats expresses nearly 100% MHC I[22]. We confirmed this finding as the male animals in the current study had 100% MHC I in the soleus muscle. However, the female animals showed a mixed distribution of MHC I and MHC IIa isoforms. MHC IIa is the most oxidative of the MHC II (fast) isoforms and it makes up less than 10% of the soleus muscle MHC content in female Sprague Dawley rats, indicating that the soleus in the female rats still has a high oxidative capacity.
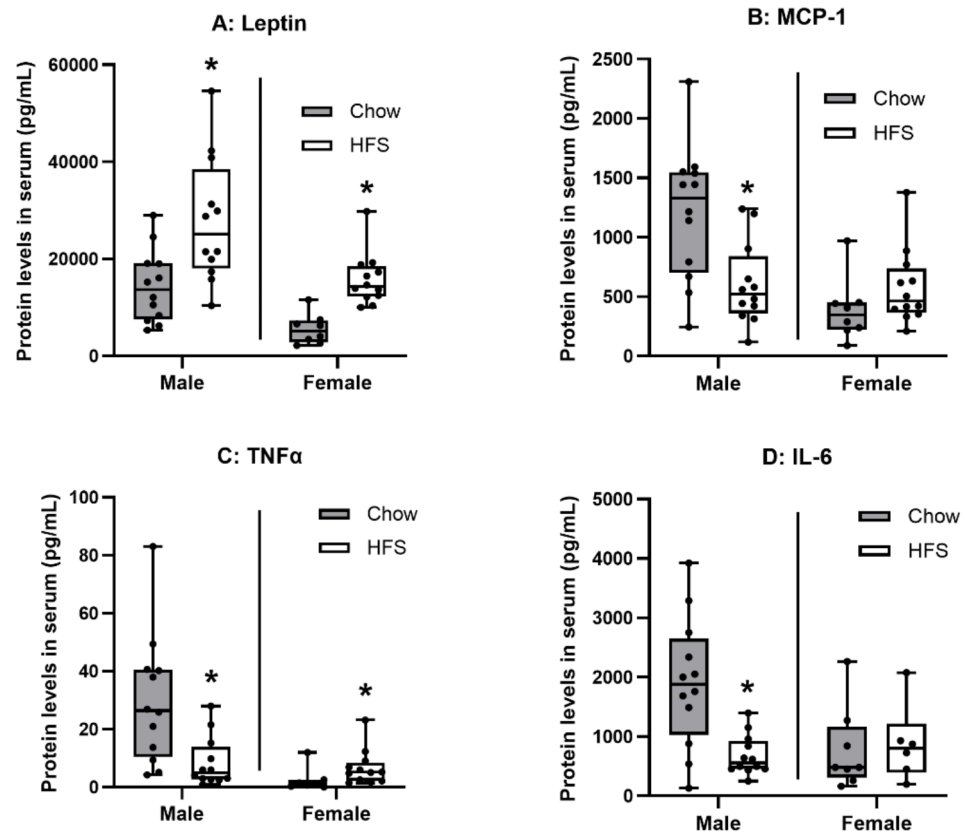
Fig. 5. Serum cytokine and adipokine levels for 24-week-old male and female rats after 12 weeks on a HFS diet and the chow control diet. *indicates statistical significance to the level of $p < 0.05$ compared to the chow-fed control animals. Data are shown in box and whisker plots.

Leptin was found to increase in both HFS diet male and female animals compared to the chow-fed controls (Fig. 5A). Leptin is a peptide hormone predominantly produced by adipocytes that influences appetite and satiety to regulate energy homeostasis[42]. Consequently, leptin levels were associated with increases in body fat percentage in both male and female animals following the HFS diet intervention period. The proinflammatory cytokines MCP-1 and IL-6 appeared to be restored to homeostatic levels for the HFS-females following the 12-week metabolic challenge (Fig. 5B,D). After 12-weeks on the HFS diet, obesity may have become a chronic condition, and a rise in inflammatory cytokines in response to the HFS diet may only occur as an acute response to the obesity-inducing diet. This has been suggested by a previous study where MCP-1 and TNFα showed an initial increase to a HFS diet but then returned to levels similar to those of the chow control group after 4 weeks[20]. In the present case however, TNFα continued to be elevated after 12 weeks on the HFS diet (Fig. 5C). This sustained increase is likely because the HFS diet has been shown to compromise the intestinal barrier thereby allowing lipopolysaccharides (LPS) to translocate into systemic circulation and induce metabolic endotoxemia[43,44]. LPS is a metabolic by-product of Gram-negative bacteria and is associated with increases in TNFα[45].

It is important to note that there was great variability in the response of the animals to the HFS diet. Sprague–Dawley rats are an outbred strain which means they have been bred to maximize genetic diversity and heterozygosity within a population. Although this likely introduced some of the variability in our results, this scenario is more representative of the human population than an inbred rat strain would be, as humans also have heterogeneous responses to diet[46]. However, small university-housed colonies, such as the one used in the current study, can experience genetic drifts, and show genetic divergence from other small colonies[47]. This may offer a possible explanation of the unusual serum cytokine results in the male animals where the chow-fed control group displayed significantly higher levels than the HFS group for almost all inflammatory markers measured (Fig. 5). This finding is in stark contrast to results reported from a similar study that observed either an increase or no change in serum inflammatory cytokines in male Sprague–Dawley rats who underwent a 4-week metabolic challenge[20].

The morphological changes of the VL muscle observed following a 12-week metabolic challenge are similar to those observed in previous studies in male Sprague–Dawley rats that found that the HFS diet was associated with an increase in fat infiltration in the VL muscle[21,23]. It has been shown previously that intramuscular fat in
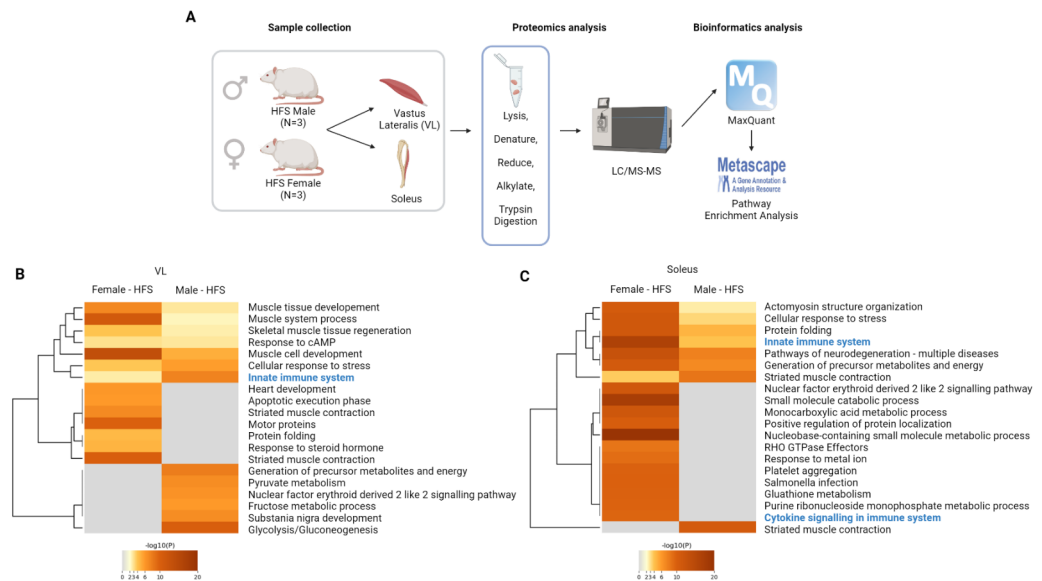
Fig. 6. Quantitative proteomics of the VL and soleus muscle of male and female Sprague–Dawley rats that have been exposed to the HFS diet for 12 weeks. (**A**) Proteomics workflow and analysis (N = 3, HFS males and N = 3, HFS females). Metascape software was used to identify pathway enrichment. A list of all detected proteins is provided in supplementary tables S1 and S2. (**B**) Metascape analysis of different pathways between HFS diet animals and Chow-fed control animals for the VL muscle. (**C**) Metascape analysis of different pathways between HFS diet and Chow-fed control animals for the soleus muscle. Blue writing indicates upregulated pathways.

the VL increases proportionally with the increase in body fat percentage[21]. Here, we confirm this result for the female VL muscle in response to the HFS diet, as there was a significant correlation between body fat and VL intramuscular fat (Fig. 4C). Surprisingly, collagen content was not significantly changed in the VL muscle in response to the HFS diet for either sex. However, this may be attributed to the length of the metabolic challenge, as increases in collagen deposition/fibrosis have been observed following 28 weeks on a HFS diet[21].

Fat is an active endocrine organ that can release inflammatory cytokines that attract proinflammatory macrophages[14,48]. Macrophage infiltration into the VL and soleus muscle in the HFS animals confirms previous findings that it seems to follow intramuscular fat infiltration, giving an indication of the local inflammatory environment. The proteomics analysis confirms the inflammation, as the innate immune system is triggered when immune cells, such as macrophages, detect tissue damage (Fig. 6). By comparing the male and female HFS diet groups of animals, we were able to determine which sex had a more pronounced inflammatory response to intramuscular fat infiltration and what specific proteins are responsible for these differences (the complete list is shown in Supplementary Tables S1-S2). We observed that males had a larger inflammatory response in the VL muscle, and females had a stronger inflammatory response to the infiltrated fat in the soleus muscle, similar to what was observed for the macrophage infiltration (Fig. 3H and I). It has been observed in certain species that females in general have a more robust and persistent immune response than males[49,50]. Specifically, it has been shown that testosterone decreases certain immune functions such as cytokine production[51,52]. The chronic inflammation involved in the immune response can have various deleterious affects on healthy tissue, putting females at a higher risk for inflammatory diseases and autoimmune conditions[53].

One of the most exciting findings of the present study is that there was a large fat infiltration in the soleus muscle of the female HFS diet group animals (Fig. 3C) compared to the males. This result detected in females is contrary to findings recorded in previous studies that suggest that the oxidative capacity of the soleus may be protective against intramuscular fat infiltration and fibrosis in male Sprague–Dawley rats[23]. A possible explanation may be offered by how males and females store fat. It is thought that estrogen mediates fat deposition preferentially away from visceral fat deposits and towards subcutaneous deposits in female rats[54]. Directing fat away from visceral deposits may make it more likely to be deposited ectopically in muscle tissues, as our data suggest that intramuscular fat infiltration in female soleus muscle also increases with body fat percentage. From an evolutionary perspective, because visceral fat contributes more to metabolic dysregulation[55], it may have been useful for females to have other mechanisms for storing fat than in the visceral region, thereby reducing the risk of disease and allowing them to care for their offspring and nurture fetuses while pregnant.

A limitation to the current study is that only mid-belly slices of both the VL and soleus were analysed. This may not be representative of the fat distribution throughout the muscle. It has been found that there are regional differences in intramuscular fat and that mid-belly fat may not necessarily be representative of whole muscle fat content[56–58]. Another limitation stems from the serum cytokine profile collected in this study. Serum cytokines are systemic markers of inflammation while local inflammation may differ from the systemic state and may give

more insight about muscle adaptation in the presence of a metabolic challenge. Results from this study call for further investigation into different muscle types and how they may be affected by obesity, as we have shown that not all muscles respond the same in the presence of a HFS diet exposure. Future studies should be aimed at quantifying the effects of a HFS diet on female sex hormones to determine the potential role of sex hormones in the regulation of fat storage.

Like humans, Sprague–Dawley rats are heterogeneous in their response to an obesity-inducing diet. In this study we illustrate similarities and differences between male and female Sprague–Dawley rats in their response to a 12-week metabolic challenge. In summary, it was found that female Sprague–Dawley rats are susceptible to obesity and show similar symptoms of metabolic disease as male rats when exposed to a HFS diet. The female animals also displayed a similar response to the diet with respect to intramuscular fat infiltration in the VL muscle. However, females receiving the HFS diet were more susceptible to intramuscular fat infiltration in the high oxidative capacity soleus muscle than males. Including females in this research may allow for a better understanding of the mechanistic relationship between diets, obesity, metabolic syndrome, and the effects of these factors on adaptation and degeneration of musculoskeletal tissues, by studying the differences in metabolic response and tissue adaptation/degeneration between the sexes.

Data availability

Data generated or analysed during this study are included in this article and supplementary information files. Additional raw proteomics data is available from the corresponding author upon request.

References

1. Shaw, D. I., Hall, W. L. & Williams, C. M. Metabolic syndrome: What is it and what are the implications?. *Proc. Nutr. Soc.* **64**(3), 349–357. https://doi.org/10.1079/pns2005442 (2005).
2. Donini, L. M. et al. Definition and diagnostic criteria for sarcopenic obesity: ESPEN and EASO consensus statement. *Obes Facts* **15**(3), 321–335. https://doi.org/10.1159/000521241 (2022).
3. Srikanthan, P. & Karlamangla, A. S. Muscle mass index as a predictor of longevity in older adults. *Am. J. Med.* **127**(6), 547–553. https://doi.org/10.1016/j.amjmed.2014.02.007 (2014).
4. Neto, L. S. S., Karnikowiski, M. G. O., Tavares, A. B. & Lima, R. M. Association between sarcopenia, sarcopenic obesity, muscle strength and quality of life variables in elderly women Associação entre sarcopenia, obesidade sarcopênica e força muscular com variáveis relacionadas de qualidade de vida em idosas. *Rev. Bras Fisioter* **16**(5), 360–367 (2012).
5. Chen, L., Nelson, D. R., Zhao, Y., Cui, Z. & Johnston, J. A. Relationship between muscle mass and muscle strength, and the impact of comorbidities: A population-based, cross-sectional study of older adults in the United States. *BMC Geriatr.* https://doi.org/10.1186/1471-2318-13-74 (2013).
6. Bosello, O. & Zamboni, M. Visceral obesity and metabolic syndrome. *Obes. Rev.* **1**(1), 47–56. https://doi.org/10.1046/j.1467-789x.2000.00008.x (2000).
7. Pan, D. et al. Skeletal muscle TMglyceride levels are inversely related to insulin action. *Diabetes* https://doi.org/10.2337/diabetes.46.6.983 (1997).
8. Therkelsen, K. E. et al. Intramuscular fat and associations with metabolic risk factors in the framingham heart study. *Arterioscler. Thromb. Vasc. Biol.* **33**(4), 863–870 (2013).
9. Addison, O., Marcus, R. L., Lastayo, P. C. & Ryan, A. S. Intermuscular fat: A review of the consequences and causes. *Int. J. Endocrinol.* https://doi.org/10.1155/2014/309570 (2014).
10. Akhmedov, D. & Berdeaux, R. The effects of obesity on skeletal muscle regeneration. *Front. Physiol.* https://doi.org/10.3389/fphys.2013.00371 (2013).
11. Kelley, D. E., Goodpaster, B., Wing, R. R. & Simoneau, J. A. Skeletal muscle fatty acid metabolism in association with insulin resistance, obesity, and weight loss. *Am. J. Physiol. Endocrinol. Metab.* **277**(6), E1130–E1141 (1999).
12. Tidball, J. G. Inflammatory processes in muscle injury and repair. *Am. J. Physiol. Regul. Integr. Comp. Physiol.* **288**, 345–353. https://doi.org/10.1152/ajpregu (2005).
13. D'Souza, D. M. et al. Diet-induced obesity impairs muscle satellite cell activation and muscle repair through alterations in hepatocyte growth factor signaling. *Physiol. Rep.* https://doi.org/10.14814/phy2.12506 (2015).
14. Fink, L. N. et al. Pro-Inflammatory macrophages increase in skeletal muscle of high fat-Fed mice and correlate with metabolic risk markers in humans. *Obesity* **22**(3), 747–757. https://doi.org/10.1002/oby.20615 (2014).
15. Mann, C. J. et al. Aberrant repair and fibrosis development in skeletal muscle. *Skelet. Muscle* https://doi.org/10.1186/2044-5040-1-21 (2011).
16. Goodpaster, B. H., He, J., Watkins, S. & Kelley, D. E. Skeletal muscle lipid content and insulin resistance: Evidence for a paradox in endurance-trained athletes. *J. Clin. Endocrinol. Metab.* **86**(12), 5755–5761 (2001).
17. Gerber, C., Schneeberger, A. G., Hoppeler, H. & Meyer, D. C. Correlation of atrophy and fatty infiltration on strength and integrity of rotator cuff repairs: A study in thirteen patients. *J. Shoulder Elbow. Surg.* **16**(6), 691–696. https://doi.org/10.1016/j.jse.2007.02.122 (2007).
18. Hilton, T. N., Tuttle, L. J., Bohnert, K. L., Mueller, M. J. & Sinacore, D. R. Excessive adipose tissue infiltration in skeletal muscle in individuals with obesity, diabetes mellitus, and peripheral neuropathy: Association with performance and function. *Phys. Ther.* **88**(11), 1336–1344 (2008).
19. Biltz, N. K. et al. Infiltration of intramuscular adipose tissue impairs skeletal muscle contraction. *J. Physiol.* **598**(13), 2669–2683. https://doi.org/10.1113/JP279595 (2020).
20. Collins, K. H. et al. A high-fat high-sucrose diet rapidly alters muscle integrity, inflammation and gut microbiota in male rats. *Sci. Rep.* https://doi.org/10.1038/srep37278 (2016).
21. Collins, K. H. et al. High-fat high-sucrose diet leads to dynamic structural and inflammatory alterations in the rat vastus lateralis muscle. *J. Orthop. Res.* **34**(12), 2069–2078. https://doi.org/10.1002/jor.23230 (2016).
22. Larson, L., Lioy, J., Johnson, J. & Medler, S. Transitional hybrid skeletal muscle fibers in rat soleus development. *J. Histochem. Cytochem.* **67**(12), 891–900. https://doi.org/10.1369/0022155419876421 (2019).
23. Collins, K. H. et al. Acute and chronic changes in rat soleus muscle after high-fat high-sucrose diet. *Physiol. Rep.* https://doi.org/10.14814/phy2.13270 (2017).
24. De Bellis, A. et al. *Gender-Related Differences in Heart Failure: Beyond the 'One-Size-Fits-All' Paradigm* (Springer, 2020). https://doi.org/10.1007/s10741-019-09824-y.

25. Golden, L. C. & Voskuhl, R. *The Importance of Studying Sex Differences in Disease: The Example of Multiple Sclerosis* (Wiley, 2017). https://doi.org/10.1002/jnr.23955.

26. Joumaa, V. et al. Effects of fiber type on force depression after active shortening in skeletal muscle. *J. Biomech.* **48**(10), 1687–1692. https://doi.org/10.1016/j.jbiomech.2015.05.023 (2015).

27. Schneider, C. A., Rasband, W. S. & Eliceiri, K. W. NIH Image to ImageJ: 25 years of image analysis. *Nat. Methods* https://doi.org/10.1038/nmeth.2089 (2012).

28. Matthews, D. R. et al. Homeostasis model assessment: insulin resistance and fl-cell function from fasting plasma glucose and insulin concentrations in man. *Diabetologia* https://doi.org/10.1007/BF00280883 (1985).

29. Waters-Banker, C., Butterfield, T. A. & Dupont-Versteegden, E. E. Immunomodulatory effects of massage on nonperturbed skeletal muscle in rats. *J. Appl. Physiol.* **116**, 164–175. https://doi.org/10.1152/japplphysiol.00573.2013.-Massage (2014).

30. Szczepanski, H. E. et al. NR4A1 modulates intestinal smooth muscle cell phenotype and dampens inflammation-associated intestinal remodeling. *FASEB J.* https://doi.org/10.1096/fj.202101817RR (2022).

31. Krawetz, R. J. et al. Mesenchymal progenitor cells from non-inflamed versus inflamed synovium post-ACL injury present with distinct phenotypes and cartilage regeneration capacity. *Stem Cell Res. Ther.* https://doi.org/10.1186/s13287-023-03396-3 (2023).

32. Das, N. et al. Tryptase β regulation of joint lubrication and inflammation via proteoglycan-4 in osteoarthritis. *Nat. Commun.* https://doi.org/10.1038/s41467-023-37598-3 (2023).

33. Gordon, M. H. et al. N-Terminomics/TAILS profiling of proteases and their substrates in ulcerative colitis. *ACS Chem. Biol.* **14**(11), 2471–2483. https://doi.org/10.1021/acschembio.9b00608 (2019).

34. Agbani, E. O. et al. Membrane procoagulation and N-terminomics/TAILS profiling in Montreal platelet syndrome kindred with VWF p.V1316M mutation. *Commun. Med.* https://doi.org/10.1038/s43856-023-00354-1 (2023).

35. Kohler, D. et al. MSstats version 4.0: Statistical analyses of quantitative mass spectrometry-based proteomic experiments with chromatography-based quantification at scale. *J. Proteome Res.* **22**(5), 1466–1482. https://doi.org/10.1021/acs.jproteome.2c00834 (2023).

36. Zhou, Y. et al. Metascape provides a biologist-oriented resource for the analysis of systems-level datasets. *Nat. Commun.* https://doi.org/10.1038/s41467-019-09234-6 (2019).

37. Collins, K. H. et al. Obesity, metabolic syndrome, and musculoskeletal disease: Common inflammatory pathways suggest a central role for loss of muscle integrity. *Front. Physiol.* https://doi.org/10.3389/fphys.2018.00112 (2018).

38. Collins, K. H. et al. Adipose tissue is a critical regulator of osteoarthritis. *PNAS* **118**(1), 1–12. https://doi.org/10.1073/pnas.2021096118/-/DCSupplemental (2020).

39. Collins, K. H. et al. Leptin mediates the regulation of muscle mass and strength by adipose tissue. *J. Physiol.* **600**, 3795–3817. https://doi.org/10.1113/JP283034 (2022).

40. Godsland, I. F., Wynn, V., Crook, D. & Miller, N. E. Sex, plasma lipoproteins, and atherosclerosis: Prevailing assumptions and outstanding questions. *Am. Heart J.* https://doi.org/10.1016/0002-8703(87)90552-7 (1987).

41. DeNies, M. S. et al. Diet-induced obesity alters skeletal muscle fiber types of male but not female mice. *Physiol. Rep.* https://doi.org/10.1002/phy2.204 (2014).

42. R. Obert *et al.*, *Serum Immunoreactive-Leptin Concentrations in Normal-Weight and Obese Humans from the Divisions of Endocrinology and Metabolism*, (Massachusetts Medical Society, 1996).

43. Cani, P. D. et al. Selective increases of bifidobacteria in gut microflora improve high-fat-diet-induced diabetes in mice through a mechanism associated with endotoxaemia. *Diabetologia* **50**(11), 2374–2383. https://doi.org/10.1007/s00125-007-0791-0 (2007).

44. Cani, P. D. et al. Changes in gut microbiota control inflammation in obese mice through a mechanism involving GLP-2-driven improvement of gut permeability. *Gut* **58**(8), 1091–1103. https://doi.org/10.1136/gut.2008.165886 (2009).

45. Jialal, I., Kaur, H. & Devaraj, S. Toll-like receptor status in obesity and metabolic syndrome: A translational perspective. *J. Clin. Endocrinol. Metab.* **99**(1), 39–48. https://doi.org/10.1210/jc.2013-3092 (2014).

46. Blüher, M. Obesity: Global epidemiology and pathogenesis. *Nat. Rev. Endocrinol.* https://doi.org/10.1038/s41574-019-0176-8 (2019).

47. Brekke, T. D., Steele, K. A. & Mulley, J. F. Inbred or outbred? Genetic diversity in laboratory rodent colonies. *G3: Genes Genomes Genet.* **8**(2), 679–686. https://doi.org/10.1534/g3.117.300495 (2018).

48. Friedman, J. M. & Halaas, J. L. Leptin and the regulation of body weight in mammals. *Nature* https://doi.org/10.1038/27376 (1998).

49. Klein, S. L. & Flanagan, K. L. Sex differences in immune responses. *Nat. Rev. Immunol.* https://doi.org/10.1038/nri.2016.90 (2016).

50. Pap, P. L., Czirják, G. Á., Vágási, C. I., Barta, Z. & Hasselquist, D. Sexual dimorphism in immune function changes during the annual cycle in house sparrows. *Naturwissenschaften* **97**(10), 891–901. https://doi.org/10.1007/s00114-010-0706-7 (2010).

51. Angele, M. K., Schwacha, M. G., Ayala, A. & Chaudry, I. H. Effect of gender and sex hormones on immune responses following shock. *SHOCK* **14**, 81–90 (2000).

52. Olsen, N. J. & Kovacs, W. J. Gonadal steroids and immunity. *Endocr. Rev.* **17**(4), 369–384 (1996).

53. Angum, F., Khan, T., Kaler, J., Siddiqui, L. & Hussain, A. The prevalence of autoimmune disorders in women: A narrative review. *Cureus* https://doi.org/10.7759/cureus.8094 (2020).

54. Kautzky-Willer, A., Harreiter, J. & Pacini, G. Sex and gender differences in risk, pathophysiology and complications of type 2 diabetes mellitus. *Endocr. Rev.* https://doi.org/10.1210/er.2015-1137 (2016).

55. S. Carobbio, V. Pellegrinelli, & A. Vidal-Puig, Adipose tissue function and expandability as determinants of lipotoxicity and the metabolic syndrome. In *Advances in Experimental Medicine and Biology*, vol. 960, 161–196. (Springer, 2017). https://doi.org/10.1007/978-3-319-48382-5_7.

56. Yoshiko, A. et al. Three-dimensional comparison of intramuscular fat content between young and old adults. *BMC Med. Imaging* https://doi.org/10.1186/s12880-017-0185-9 (2017).

57. Vidt, M. E. et al. Assessments of fatty infiltration and muscle atrophy from a single magnetic resonance image slice are not predictive of 3-dimensional measurements. *Arthrosc. J. Arthrosc. Relat. Surg.* **32**(1), 128–139. https://doi.org/10.1016/j.arthro.2015.06.035 (2016).

58. Biltz, N. K. & Meyer, G. A. A novel method for the quantification of fatty infiltration in skeletal muscle. *Skelet. Muscle* https://doi.org/10.1186/s13395-016-0118-2 (2017).

Acknowledgements

Author contributions

H.E.S. was responsible for data collection, analysis, interpretation, drafting the manuscript, revising the manuscript, and approving the final version. N.A. and R.A.S. contributed to the execution of the study and data collection and analysis. F.S. and D.Y. contributed to the data collection and analysis. A.D., R.A.R., and D. A. H. contributed to the interpretation of data, revising the manuscript, and approving the final version. W.H. was

responsible for design of the study, data analysis, interpretation of data, revising the manuscript, and approving the final version.

Declarations

Competing interests
The authors declare no competing interests.

Additional information
Supplementary Information The online version contains supplementary material available at https://doi.org/10.1038/s41598-024-85084-7.

Correspondence and requests for materials should be addressed to H.E.S. or W.H.

Reprints and permissions information is available at www.nature.com/reprints.

Publisher's note Springer Nature remains neutral with regard to jurisdictional claims in published maps and institutional affiliations.